Intellectual Merit. Heat extraction from the Earth via hydrothermal systems along mid-ocean ridges (MORs) is a fundamental process affecting the Earth: hydrothermal systems extract approximately one third of the global yearly heat loss through ridges and are a primary means of chemical exchange between the solid Earth and the oceans. It is generally believed that sections of MORs with greater magma supply host a greater abundance of hydrothermal systems. While this simple conceptual model provides a framework within which to understand hydrothermal heat generation, the relative roles of magmatic heat input, tectonic heat advection, and faulting in controlling ridge thermal structure and hydrothermal circulation are still poorly understood. This is particularly important for hydrothermal circulation at slow- and ultra-slow spreading ridges, where venting occurs in a variety of host-rock lithology and tectonic setting. The Rainbow hydrothermal field (RHF) is a methane-, hydrogen- and iron-rich system located on an ultramafic massif within a tectonized non-transform discontinuity (NTD) of the Mid-Atlantic Ridge, where current models predict that long-term magma supply should be very low. Yet Rainbow vents high-temperature fluids at high flow rates, which is difficult to explain without a magmatic heat source. This conundrum stands in the way of our ability to develop general models for the roles of magmatic heat input and tectonic faulting on controlling ridge thermal structure and hydrothermal circulation, particularly for hydrothermal systems located in regions dominated by ultramafic lithologies, which are common at slow and ultra-slow MORs. We propose a three-part seismic study of the physical architecture of the crustal and upper mantle at Rainbow to address the following fundamental question: **What is the relationship between magmatism, faulting, substrate lithology, and hydrothermal circulation at the Rainbow hydrothermal field?** A combination of 3D and 2D high-resolution active-source seismic tomography, 2D multichannel seismic reflection, and passive microearthquake monitoring will allow us to determine the tectonic and thermal structure, melt content, and microseismicity around and beneath the RHF to test specific hypotheses concerning:

- *The nature and location of the heat source driving hydrothermal circulation at RHF:* is the NTD experiencing an unusual period of enhanced melt supply from the mantle, or are fluids extracting heat from the magmatic systems of the neighboring spreading segments?
- *The nature and origin of the Rainbow massif:* is the Rainbow massif predominantly ultramafic, or does it have a mafic component? Is detachment faulting responsible for the uplift of the massif, or does buoyancy from mantle serpentinization play a role?
- *The role of the local stress field on focusing hydrothermal discharge:* does detachment-faulting control the focusing of hydrothermal fluids? What are the linkages between the different sets of faults and lineaments that crosscut the massif with the geometry/location of the heat source and the hypothetical detachment fault?

Investigation of the subsurface structure of this unique system will advance understanding of how high-temperature hydrothermal fluids can be generated in tectonized, ultramafic terrains, and to make predictions about how common similar hydrothermal systems (i.e., hosted in ultramafic rocks, venting hydrogen, methane, and iron-rich high-temperature fluids) might be along other slow- and ultra-slow spreading ridges. Our results will inform fundamental problems in MOR geochemistry, fluid chemistry, and geo-microbiology

Broader Impacts. Our results will mesh well with data collected as part of the international InterRIDGE and NSF's RIDGE2000 programs. The data sets we propose to collect are substantive and will be made available to the broader community via the IRIS data management center, providing productive research in many areas for years to come. Development of human resources in the form of graduate and undergraduate student training is an important outgrowth of this proposal. This study will form part of the Ph.D. thesis research projects of UH-SOEST and MIT/WHOI Joint Program graduate students, who will be trained in various seismic disciplines. The PIs will incorporate undergraduate interns in several aspects of the work. These students will gather and analyze data and will be introduced to earthquake analysis and seismic imaging methods.

Collaborative Proposal: Seismic Investigation of the Rainbow Hydrothermal Field and its Tectono/Magmatic Setting, Mid-Atlantic Ridge 36° 14'N

1. Introduction and Motivation

Heat extraction from the Earth via hydrothermal systems along mid-ocean ridges (MORs) is a fundamental process affecting the Earth: hydrothermal systems extract approximately one third of the global yearly heat loss through ridges and are a primary means of chemical exchange between the solid Earth and the oceans. Hydrothermal circulation occurs when seawater penetrating the lithosphere through fractures is heated through its contact with hot rock, undergoing chemical alteration. As it penetrates deeper, its temperature increases and the water becomes buoyant, rapidly rising back to the seafloor. Sections of MORs with greater magma supply, and hence greater heat flux, are thought to host a greater abundance of hydrothermal systems. This simple conceptual model provides a framework within which to understand hydrothermal heat generation and extraction, yet leaves open the question of the nature of heat sources and the physical mechanisms controlling hydrothermal fluid flow [e.g., *Wilcock and Delaney*, 1996].

Most of our understanding of hydrothermal systems along ridges results from studies of the materials output by this process [e.g., *Humphris et al.*, 1995; *Von Damm*, 1990]. In contrast, the deeper distributions of melt that may drive these systems and the general tectonic and thermal structure around them are inadequately known and have been studied in only a few locations, most of them along fast and intermediate spreading ridges like the East Pacific Rise and the Juan de Fuca Ridge. In these settings, hydrothermal systems are mainly located within the axial zone of a spreading segment, hosted in basaltic rock, and are primarily driven by heat extracted from crystallization of mid-crustal melt sills [e.g., *Canales et al.*, 2006; *Haymon et al.*, 1991; *Singh et al.*, 1998; *Van Ark et al.*, 2007]. In contrast, hydrothermal systems along slow spreading ridges like the Mid-Atlantic Ridge (MAR) show a great variety of venting styles and host-rock lithology, and are located in diverse tectonic settings like axial volcanic ridges, non-transform ridge discontinuities (NTDs), the foot of ridge valley walls, and off-axis inside corner highs [e.g., *German and Lin*, 2004; *German and Parson*, 1998]. Here the relative roles of magmatic heat input, tectonic heat advection, and faulting in controlling ridge thermal structure and hydrothermal circulation are still poorly understood [e.g., *Cannat et al.*, 2004].

The Rainbow hydrothermal field (RHF) is a major high-temperature hydrothermal system that is located within one such setting, a non-transform discontinuity of the MAR [*German et al.*, 1996]. It is hosted in an ultramafic massif, venting methane-, hydrogen- and iron-rich fluids [e.g., *Holm and Charlou*, 2001] that support diverse macrofaunal and microbial communities [e.g., *Desbruyères et al.*, 2001; *O'Brien et al.*, 1998]. The tectonized setting of the NTD lacks significant volcanic features, yet the RHF vents high-temperature fluids (up to 365 °C) at high flow rates [*German et al.*, 1996], which is difficult to explain without a magmatic heat source. This conundrum stands in the way of our ability to develop a model for the origin and functioning of the Rainbow vent field as well as inhibits development of more general models for the roles of magmatic heat input and tectonic faulting on controlling thermal structure and hydrothermal circulation, particularly for hydrothermal systems in regions dominated by ultramafic lithologies, which are common at slow and ultra-slow MORs [e.g., *Cannat et al.*, 1995; *Dick et al.*, 2003].

The fundamental question we aim to address is: **What is the relationship between magmatism, faulting, substrate lithology, and hydrothermal circulation at the Rainbow hydrothermal field?** We will answer this question by testing a specific hypothesis against two alternates:

Hypothesis: *The heat driving hydrothermal circulation at Rainbow is provided by a magma body underlying the ultramafic rocks exposed on the massif, and steep normal faults crosscutting the massif provide permeability pathways for fluid circulation*. If this hypothesis is correct, then Rainbow may be experiencing a phase of enhanced melt supply from the mantle, therefore providing an excellent

opportunity to investigate delivery and emplacement of melt beneath a NTD, where long-term magma supply should be very low [e.g., *Cannat et al.*, 1995; *Phipps Morgan and Forsyth*, 1988]. In addition, this hypothesis predicts that at least part of the Rainbow massif could be mafic in origin, despite indications suggesting is predominantly ultramafic [e.g., *Fouquet et al.*, 1997].

Alternative 1: *The heat driving hydrothermal circulation at Rainbow is extracted from the magmatic system(s) of the neighboring segment(s), and fluids are transported relatively large lateral distances on possibly low-angle fault(s).* An alternative to hypothesis 1 is that the NTD is currently magmatically starved, but fluids are taping magmatic heat from the neighboring segments [*German et al.*, 1996], possibly via low-angle faults that provide pathways for fluids to travel from the ends of the neighboring segments to the center of the NTD. Thus, this hypothesis does not require presence of a significant component of mafic lithologies beneath the massif, consistent with seafloor observations and exit fluid chemistry.

Alternative 2: *Detachment faulting controls hydrothermal circulation and uplift of the Rainbow massif*. There is increasing evidence that a variety of hydrothermal venting styles are intimately linked to detachment faulting and formation/evolution of oceanic core complexes [*McCaig et al.*, 2007]. It has been proposed that the RHF sits on the footwall of a detachment fault [*Gràcia et al.*, 2000], and some of the geological characteristics of the massif are consistent with this hypothesis [*Gaill et al.*, 2007; *Ildefonse et al.*, 2008]. In this scenario fluids could extract heat from the hot (and possibly molten) deep region of the mantle where a detachment fault roots, and/or from the exhuming footwall. If uplift of the massif is not the result of detachment faulting, then buoyant diapirism driven by serpentinization is a likely alternative [e.g., *Bonatti*, 1976], as substantial hydration of the mantle beneath the massif would be accompanied by volumetric expansion and reduced density.

To test these hypotheses we propose to carefully image the subsurface architecture (which is intimately linked to hydrothermal flow processes) around and beneath the RHF and map, in 3D, the seismicity associated with the vent field and the NTD. A combination of large-scale 3D and 2D high-resolution active-source seismic tomography, 2D multichannel seismic reflection profiling, and passive microearthquake monitoring, is the most promising approach to successfully resolve the physical architecture of the crust and upper mantle at Rainbow.

Investigation of the subsurface structure of this unique system will advance understanding of the relationships between magmatic processes, hydrothermal circulation, and the thermal and tectonic structure of a ridge discontinuity, which will be applicable to other regions. In particular, understanding the mechanisms and processes that result in hydrothermal circulation at Rainbow will allow us to understand how high-temperature hydrothermal fluids can be generated in tectonized, ultramafic terrains (e.g., Logatchev and Ashazde fields in the MAR [*Bel'tenev et al.*, 2005; *Krasnov et al.*, 1996]), and to make predictions about how common similar hydrothermal systems (i.e., hosted in ultramafic rocks, venting hydrogen, methane, and iron-rich high-temperature fluids) might be along other slow- and ultra-slow spreading ridges. Our results will mesh well with data and results collected as part of the international InterRIDGE program (Rainbow is one of the two study areas of the MoMAR initiative: www.momar.org), and they will inform fundamental problems in MOR geochemistry, fluid chemistry, and geo-microbiology.

2. The Rainbow Area (MAR 36°14'N)

The MAR between the Azores triple junction and the Oceanographer FZ shows abundant indications of hydrothermal activity [*German and Parson*, 1998]. The RHF is one of several that have been discovered in recent years in this area, which also includes the active high-T sites of Lucky Strike [*Langmuir et al.*, 1997] and Menez Gwen [*Fouquet et al.*, 1995], and the low-T sites of Saldanha [*Barriga et al.*, 1998] and Menez Hom [*Fouquet et al.*, 2002] (**Figure 1**). Many of these systems seem to be hosted in ultramafic

rocks, particularly those located within NTDs, as indicated by the elevated concentrations of CH_4 and low levels of dissolved manganese detected in hydrothermal plume surveys [*Gràcia et al.*, 2000]. The intense faulting and fracturing within NTDs may favor water circulation, mantle serpentinization, and hydrothermal circulation.

The RHF, located in the MAR near 36°14'N within a NTD with relatively small offset (<25 km), was first located using acoustic seafloor imaging and water-column surveys [*German et al.*, 1996]. Subsequent submersible observations determined the geological context of the site [*Fouquet et al.*, 1997], and recent expeditions led by French investigators have studied in detail the geology of the area [*Dyment et al.*, 2008; *Gaill et al.*, 2007; *Gente et al.*, 2008; *Ildefonse et al.*, 2007a, 2008]. The hydrothermal field is located on the western flank of a massif that has some of the geological characteristics commonly associated with oceanic core complexes (OCCs) such as domed morphology and exposures of lower crustal and upper mantle lithologies [*Gaill et al.*, 2007; *Ildefonse et al.*, 2008], although no evidence has been found for the low-angle detachment fault that is also commonly associated with OCCs [*Gente et al.*, 2008].

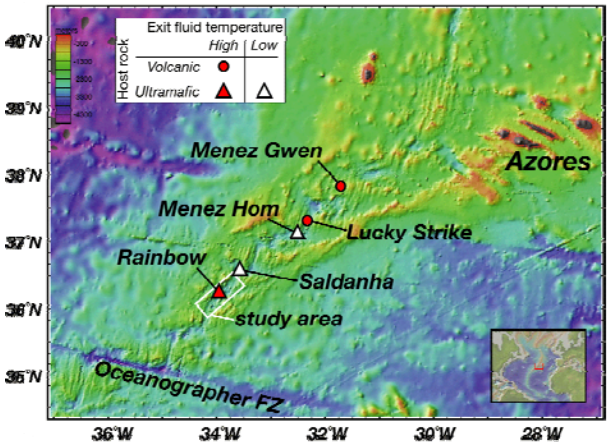

Fig. 1. Bathymetry of the MAR and its flanks between the Azores triple junction and the Oceanographer FZ. The study area and other known active hydrothermal fields are labeled.

A thick sedimentary cover prevents extensive geological mapping and dredging, but basement lithologies are exposed at some fault scarps and have been dredged and sampled from submersibles (**Figure 2**). Abundant peridotite (harzburgite and dunite) with a variety of serpentinization styles and intensity are present in the NW, N, and NE flanks of the massif. Gabbros have been sparsely sampled, and some fresh basaltic glasses have been recovered from talus and sediments on the SW and NE flanks of the massif [*Gaill et al.*, 2007; *Ildefonse et al.*, 2008] (**Figure 2**). The massif is highly tectonized by normal faults along different directions. The general tectonics is dominated by a set of N-S trending faults along the W flank, and a series of SW-NE ridges on the NE flank [*Gente et al.*, 2008; *Ildefonse et al.*, 2008]. *Gràcia et al*. [2000] points out that the Rainbow massif is located at the zone of maximum extension within the NTD caused by horizontal shear stresses due to differential spreading between the segments of the north and to the south [*Grindlay and Fox*, 1993; *Grindlay et al.*, 1991] (**Figure 3**). Within this complex tectonic setting, detachment faulting and uplifting of mantle rocks may occur if magma budget is low, particularly during periods of segment retreat [*Gràcia et al.*, 1997].

The hydrothermal field is located on the W flank of the massif, where the N-S trending fault pattern and the SW-NE trending ridges crosscut [*Gente et al.*, 2008; *Ildefonse et al.*, 2008] (**Figure 2**). The field is mainly composed of 10 black smoker chimneys and several other active and inactive vents occupying a ~200 m by ~100 m area. Exit fluid temperatures from the chimneys are up to 365 °C, and fluids exhibit low pH, interpreted as resulting from interaction with ultramafic rocks. This interaction of water with the mantle substrate results in serpentinization of the ultramafic rocks, which is an exothermic reaction. It has been argued that the energy extracted from serpentinization can drive low temperature hydrothermal systems like the Lost City field at Atlantis Massif [*Früh-Green et al.*, 2003], although there is no consensus about the efficiency of serpentinization to drive such systems [e.g., *Allen and Seyfried*, 2004]. The high fluid temperatures and large flow rates measured at the Rainbow site [*Thurnherr and Richards*, 2001] are difficult to explain by mineralization reactions [*Allen and Seyfried*, 2004], suggesting that hydrothermal circulation at Rainbow must be driven by heat extracted from crystallizing magma body(s).

Hydrothermal plume-flux studies at Rainbow indicate a power output of 0.5-3.1 GW [*Thurnherr and Richards*, 2001; *Thurnherr et al.*, 2002] which *German and Lin* [2004] use to estimate that hydrothermal activity at Rainbow has been sustained over the last ~10,000 yr, requiring an extremely high energy input of $7.3 \cdot 10^{20}$ J. According to these authors, mining that amount of energy would require fluids venting out of Rainbow to extract energy from a ~250-500 km section of the ridge if all heat was extracted from the upper ~2 km of the crust, or from a ~25-150-km-long section if fluid circulation penetrates as deep as ~6 km. The upper bounds of these calculations seem highly unrealistic. Therefore it is more likely the fluid circulation beneath Rainbow is occurring within an area of ~<25 km in diameter and at least as deep as 6 km, but probably deeper. In any case this still poses a problem for our current thinking because it is not expected that magma supply from the mantle within NTDs can be sustained over long periods of time in such a broad zone. Our experimental approach will target both the maximum depth of fluid circulation beneath Rainbow and the presence and lateral extent of magma body(s) and/or anomalous hot rock providing heat to the system.

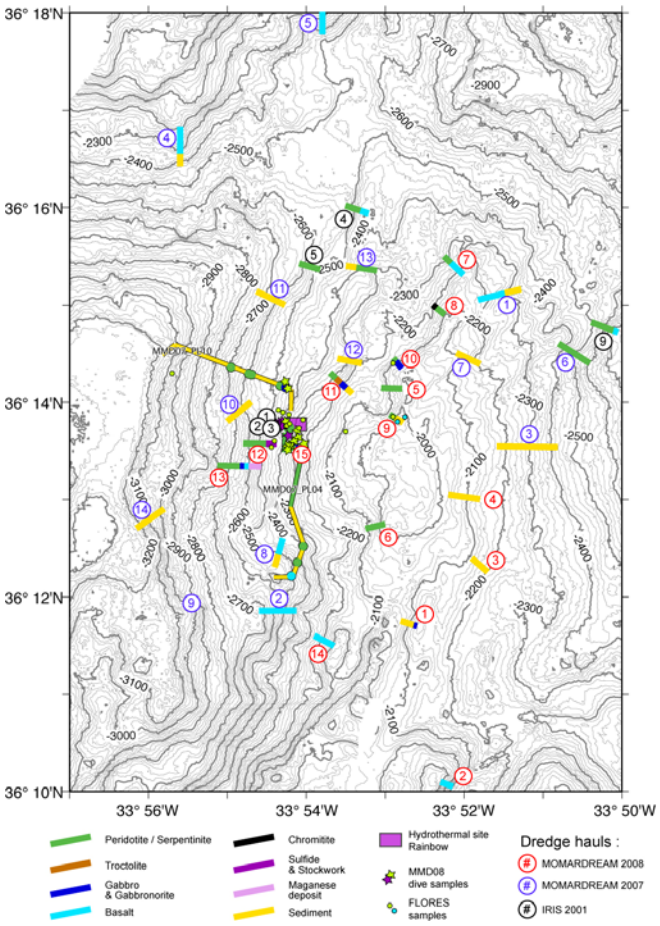

Fig. 2. Bathymetry of the Rainbow massif and sampled lithologies (dredges and submersible). Figure courtesy of B. Ildefonse, Y. Fouquet, and J. Dyment (unpublished data).

3. Magma Supply and Hydrothermal Circulation within a NTD: Specific Hypotheses to Test

There is circumstantial evidence for a magmatic source for the RHF, but there are very few specific hypotheses about its nature, location, geometry, or relation to the underlying mantle [e.g., *German et al.*, 1996]. In addition, the mechanism that formed or uplifted the Rainbow massif, and its relationship to hydrothermal circulation are not understood. Recent studies addressing tectonic denudation by detachment faulting and its relation to hydrothermal flow [e.g., *deMartin et al.*, 2007; *McCaig et al.*, 2007] allow us to envision three plausible scenarios for the nature of the heat source of the RHF and the origin and nature of the Rainbow massif. Here we briefly summarize those scenarios, highlight the testable hypotheses that our study will address, and discuss the implications for global MOR processes.

3.1. Nature and location of the heat source driving the Rainbow hydrothermal field.

Geophysical and geological observations, and numerical models of mantle flow indicate that the time-integrated supply of magma from the mantle beneath NTDs is lower, on average, than beneath slow-spreading segment centers [e.g., *Canales et al.*, 2000; *Cannat et al.*, 1995; *Lin et al.*, 1990; *Phipps Morgan and Forsyth*, 1988]. However we know that NTDs do experience episodic magmatism because basalts and volcanic features, although not common, are found within ridge discontinuities [e.g., *Tucholke and Lin*, 1994]. Magmatic heat input is required to sustain high-T hydrothermal circulation over long

periods of time [e.g., *Cann et al.*, 1985]. Global trends of hydrothermal activity indicators show a positive correlation with magma-budget proxies, even for slow-spreading ridges such as the MAR [*Baker and German*, 2004]. These simple concepts thus predict that high-T hydrothermal activity within NTDs should be rare, sporadic, and short-lived. Thus the mere existence of the Rainbow hydrothermal field allows to hypothesize that this particular NTD is going through an unusual magmatic phase, providing a unique opportunity to study the delivery and emplacement of melt from the mantle within a ridge segment discontinuity.

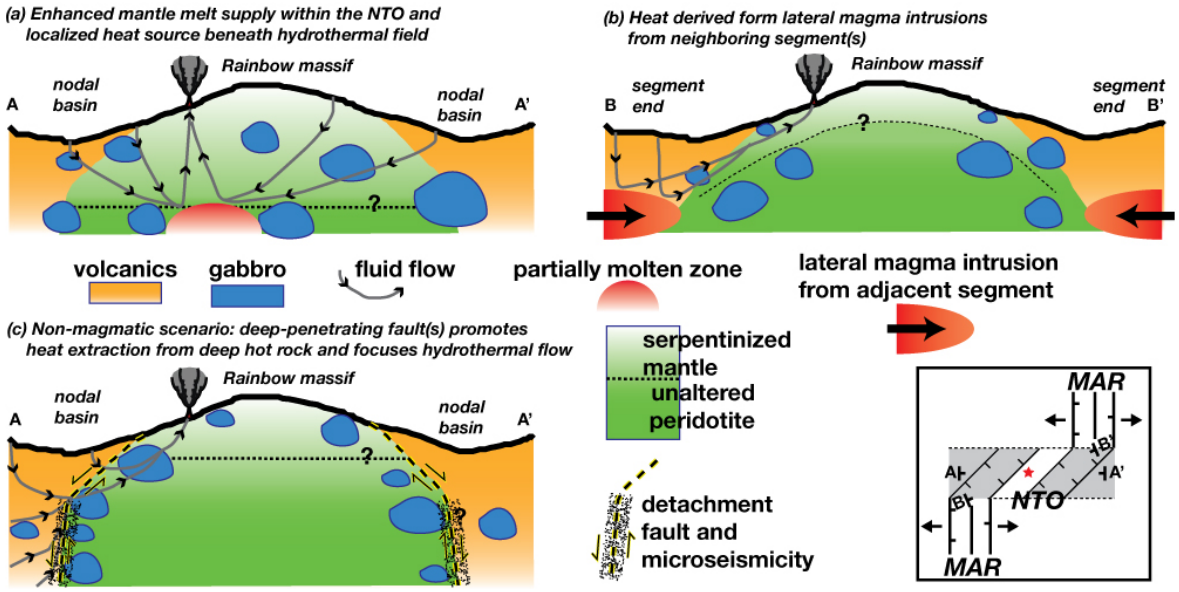

Fig. 3: Plausible models for heat extraction at the RHF. These models are inspired from and include features of the models of *German et al*. [1996], *Gràcia et al*. [2000], *Escartín et al.* [2003], *deMartin et al.* [2007], and *McCaig et al.* [2007]. Cartoons are not drawn at any particular scale because of the uncertainty on the depth of the heat source and extent of hydrothermal circulation. (a) Magma intrusion from the mantle directly beneath the RHF. In this scenario hydrothermal circulation occurs within most of the Rainbow massif, resulting in large volumes of serpentinization that contribute to buoyancy and uplifting of the massif. (b) Fluids extract heat from magma intrusions fed laterally from the neighboring segments. (c) The Rainbow massif is uplifted along a (set of) deep-penetrating detachment fault(s). Fluids extract heat from a deep region and/or hot gabbros emplaced with the exhuming footwall, and are focused along the detachment fault. Inset shows a simplified tectonic model for the formation of the Rainbow massif [*Gràcia et al.*, 2000].

Our working hypothesis is that melt is being delivered from the mantle directly within the NTD and beneath the Rainbow massif (**Figure 3a**). The presence of fresh basalt glasses on the flanks of the massif [*Ildefonse et al.*, 2008] (**Figure 2**) provides some support for this hypothesis. In this scenario, the tectonized setting of the massif allows water to penetrate and extract heat from the crystallizing magma body(s). If this hypothesis is true, our experiment will confirm the presence of magma and higher-than-background temperatures by detecting a seismic low velocity zone and/or by imaging reflections form a melt sill beneath the massif. The global implications, and predictions, of this hypothesis is that Rainbow-like hydrothermal systems (i.e., high-T systems within an ultramafic NTD) should be very uncommon along slow and ultra-slow spreading centers because they require enhanced melt supply from the mantle beneath an NTD, a process that current models agree is episodic through geological time scales.

An alternative scenario is that the Rainbow NTD remains in a magmatically-starved stage, and that hydrothermal circulation is being driven by heat extracted from the magmatic system(s) of one (or both) of the neighboring segments, with magma being injected laterally into the NTD form one of the neighboring segments (**Figure 3b**). *German et al.* [1996] propose this as a plausible hypothesis for

Rainbow based on the observation of a neovolcanic zone in the segment to the south ~15-20 km away. This scenario predicts a seismic structure very different from the previous one; our experiment will test whether or not the segment ends bounding the Rainbow NTD are associated with low seismic velocities attributable to presence of melt and elevated temperatures. If this scenario turns out to be true, then the global implication and prediction is that fault systems are capable of transporting hydrothermal fluids large lateral distances from the magma reservoirs that provide the heat to drive high-temperature convection, and that Rainbow-like hydrothermal systems within NTDs may not be uncommon along slow-spreading ridges as it seems (provided that magmatism in the neighboring segments is robust enough).

A third plausible and testable scenario is that hydrothermal circulation at Rainbow is controlled by, and related to, detachment faulting and OCC formation [*McCaig et al.*, 2007] (**Figure 3c**). It has been proposed that Rainbow sits on the footwall of a detachment fault [*Gràcia et al.*, 2000], and the domed shape of the Rainbow massif and the exposures of deep crustal and upper mantle lithologies are consistent with this hypothesis [*Gaill et al.*, 2007; *Ildefonse et al.*, 2008]. There is increasing evidence that detachment faults (or at least some of them) nucleate in a hot or partially molten region that provides the adequate rheological boundary [e.g., *Dick et al.*, 2000; *Escartín et al.*, 2003]. These so-called "hot detachments" may favor emplacement of hot gabbro plutons within the footwall, consistent with deep drilling at exposed detachment faults [*Blackman et al.*, 2006; *Dick et al.*, 2000; *Kelemen et al.*, 2004] and seismic observations [*Canales et al.*, 2008]. Fluids percolating down within the nodal basin(s) could extract heat by tapping this hot, possibly molten, deep region of the mantle where the detachment fault roots, and/or from the hot footwall [*McCaig et al.*, 2007]. Our microseismicity study will test this detachment fault hypothesis [*deMartin et al.*, 2007], it will delineate the shape of the detachment fault(s), and provide constraints on the maximum depth of hydrothermal circulation. This detachment fault hypothesis does not require enhanced magma supply to the NTD, and detachment faulting is being recognized as a fundamental mode of lithospheric accretion that may operate along ~50% of slow and ultra-slow spreading segments [*Escartín et al.*, 2008; *Smith et al.*, 2006]. Therefore, if we confirm that high-temperature venting at Rainbow is controlled by and related to detachment faulting, the global implication of this finding would be that Rainbow-like hydrothermal systems are probably much more common within slow-spreading segment discontinuities and along ultra-slow spreading centers than previously thought. This could have important implications for geochemical cycles and geo-biology because of the elevated concentrations of hydrogen, methane and iron that characterize fluids in these systems.

3.2. Nature and origin of the Rainbow massif.

The different scenarios and hypotheses outlined above have also implications for the nature and origin of the Rainbow massif. On the basis of seafloor sampling and vent fluid chemistry there seems to be consensus among researches that Rainbow is a predominantly ultramafic massif [e.g., *Charlou et al.*, 2002; *Fouquet et al.*, 1997]. However the possibility that at least part of the massif is mafic in origin cannot be excluded yet. Previous experience indicates that although ultramafic rocks might be common on the seafloor at OCCs like Atlantis massif [e.g., *Blackman et al.*, 2002], OCCs are commonly characterized by intrusive, massive gabbro plutons [e.g., *Blackman et al.*, 2006; *Canales et al.*, 2008; *Ildefonse et al.*, 2007b]. The presence of basalts and some gabbro at Rainbow (**Figure 2**) suggest that the contribution of mafic lithologies to the internal structure of the massif remains to be explored.

In addition to the composition of the massif, it is important to understand the mechanism for its uplift or emplacement. The detachment fault model (**Figure 3c**) provides a simple explanation for the dome shape of the massif and its elevation from the surrounding seafloor: extension along a detachment fault results in uplift and flexural rotation of the footwall [e.g., *Buck*, 1988]. Alternatively, Rainbow massif could be the result of buoyant diapirism promoted by serpentinization [e.g., *Bonatti*, 1976]. Hydration of mantle

peridotite results in volumetric expansion and reduced density [e.g., *Coleman*, 1971]. The hypothesis that magma emplacement beneath the Rainbow massif drives high-temperature hydrothermal circulation (**Figure 3a**) implies that hydration of the massif might be pervasive and extensive because serpentinization is very efficient at temperatures of 100-300 °C [*Macdonald and Fyfe*, 1985]. Thus magma emplacement within an ultramafic NTD can drive high-temperature hydrothermal circulation, which in turn could result in large volumes of low-density hydrated ultramafic rocks above the level of magma emplacement that ultimately rise as a buoyant diapir. Our seismic experiment is designed to be able to distinguish among those major lithological units (volcanic, gabbros, serpentinites), as we have done recently in other MAR settings [*Canales et al.*, 2008; *Xu et al.*, 2009]. In combination with the microseismicity monitoring, it will allow us to distinguish between different mechanism for the formation of the Rainbow massif: tectonic unroofing, serpentinite diapirism, or magmatic construction.

3.3. Role of local stress field on focusing hydrothermal discharge.

The RHF is located at the intersection between two major tectonic patterns: a set of N-S trending faults along the W flank, and a series of SW-NE ridges on the NE flank [*Gente et al.*, 2008; *Ildefonse et al.*, 2008]. This confluence of stress regimes and fault zones may enhance permeability of the crust and focus hydrothermal discharge. However the relation between this local stress fields and the subsurface architecture is unknown. We will explore the linkages between the different sets of faults and lineaments that crosscut the massif with the geometry/location of the heat source and the hypothetical detachment fault to better understand the relative roles of magmatism, large-scale faulting and local tectonics in controlling and focusing hydrothermal flow.

Our proposed experiment, outlined below, incorporates three different seismic techniques within one study and has been carefully designed to determine the tectonic structures, thermal structure, and melt distribution at the Rainbow site and to test these major hypotheses by answering the related questions.

4. Proposed Data Collection

Our principal scientific objective is to determine how melt supply, deep thermal structure, and/or ridge crest tectonic structures and processes are related to hydrothermal output at the RHF. The highest resolution constraints on overall crustal and thermal structure and melt content in the crust and upper mantle can be obtained by integrating three different geophysical approaches: high-resolution active-source tomographic imaging [e.g., *Dunn et al.*, 2000, 2001, 2005], multi-channel seismic studies [e.g., *Singh et al.*, 2006], and microseismicity studies [e.g., *deMartin et al.*, 2007]. A seismic study of Rainbow that incorporates active-source large-scale 3-D seismic tomography, high-resolution 2-D tomography at shallow levels, and MCS reflection imaging is essential for a successful imaging study that can achieve the desired resolution of sub-surface structure (**Figure 4**). In conjunction with the active-source imaging, our proposed microearthquake study of the region will delineate the set of faults that control the tectonics of the Rainbow massif and provide major pathways for hydrothermal circulation, and constrain the depth of brittle-ductile transition, thereby providing an independent measure of the thermal structure.

The goals of the experiment include:

(1) Provide 3-D P-wave tomographic images of the Rainbow vent area and its surroundings, with enhanced resolution near the main vent field. We propose to tomographically map the seismic velocity structure of the lithosphere beneath a 70-km-long and 30-km-wide section of the Mid-Atlantic Ridge (**Figure 4**). We will obtain dense subsurface sampling with refractions and wide-angle reflections that will enable us to image a large volume of the structure beneath the seafloor and determine melt content, thermal distribution, and stress-induced cracking (via anisotropy). Beneath the depth where most cracks are closed by the effect of pressure, we will measure the orientation and magnitude of anisotropy in the uppermost mantle and estimate the general mantle flow pattern - providing information on the

relationship between mantle flow and the tectonics of the NTO. Wide-angle reflections recorded on the OBS will complement the MCS dataset. We will be particularly interested in any reflections from what may be deduced as the transition from shallow hydrothermally altered mantle to unaltered mantle.

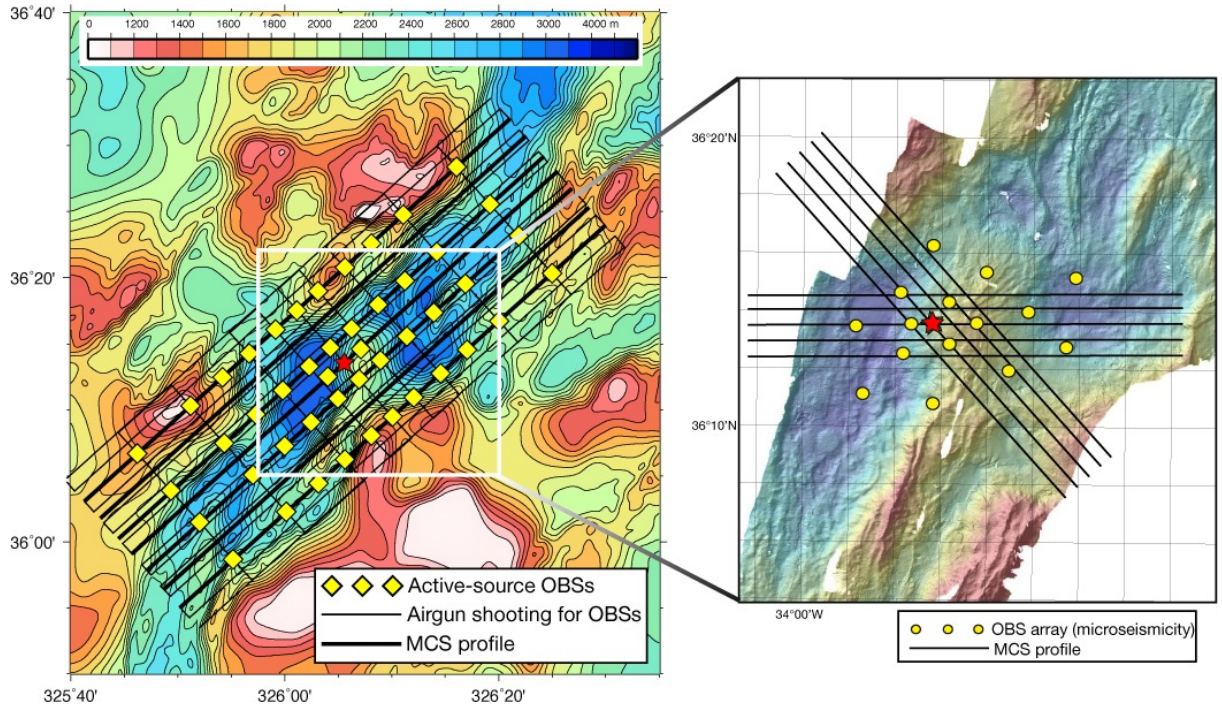

Fig. 4. Seafloor bathymetry of the MAR Rainbow area and the layout of the proposed multi-component seismic experiment. Red star is the RHF. Left: yellow diamonds indicate OBS locations for active-source recording. Airgun lines are show as thin black lines (3D OBS tomography lines) and thick black lines are MCS profiles for 2D streamer tomography. Right: yellow circles indicate locations of OBS for the micro-earthquake study. Black lines are MCS profiles. High-resolution bathymetry map on the right courtesy of Y. Fouquet, B. Ildefonse, and J. Dyment (unpublished data).

We have designed an array of 46 short-period OBSs that features closely spaced instruments within a large grid centered on the main vent field; airgun shots will occur along ridge parallel and perpendicular lines. The wide grid of OBSs is necessary to penetrate as deeply as possible beneath the seafloor[1]. Ocean bottom seismometers have improved greatly in recent years: the new OBSIP short-period instruments have four components (three seismometer and one hydrophone channel), high sampling rates, low noise levels, wide dynamic range, and high instrument recovery rates (>95%). On the basis of our experience with previous 3-D tomography [e.g., *Dunn et al.*, 2000, 2001, 2005; *Dunn and Toomey*, 1997] and preliminary resolution tests (**Figure 5**), the proposed geometry will provide a dense coverage of intersecting ray paths from a broad range of angles that will allow us to image 3-D structure on a scale of 0.5-1 km at depths of ~1.5-4 km and 2-4 km at greater depths (up to ~10-15 km depth at most). At shallower depths (<2 km), resolution will be improved by incorporating the constraints obtained from shallow 2-D streamer tomography (next section).

[1] Note to reviewers: the orientation of the 3D box is oblique to the spreading direction and general MAR trend because is the most efficient geometry to image simultaneously the NTD and the ends of the neighboring segments. To image those features with a more N-S or E-W oriented box would require a much larger number of sources and receivers, increasing costs without clear benefits. In addition, the 3D nature of the OBS experiment will make the obliqueness between shooting lines and structures not an issue for modeling and interpretation.

(2) Obtain high-resolution seismic reflection images and 2-D seismic velocity models of the uppermost lithosphere (<2-2.5 km) using long-offset (8 km) MCS streamer data. We propose to acquire two sets of MCS profiles using an 8-km-long hydrophone streamer towed behind the ship. The first set of 7 80-km-long SW-NE MCS profiles (coincident with the long OBS shooting profiles[2], **Figure 4-left**) will be primarily used for 2D high-resolution streamer travel-time tomography. Shallow seismic refractions observed in the streamer data will be modeled using 2-D travel-time tomography methods [e.g., *Calvert et al.*, 2003; *Canales et al.*, 2008; *Zelt et al.*, 2004] to complement the 3-D large-scale velocity models. One of our co-P.I.s has recently applied successfully this type of analysis to MCS data collected with a shorter streamer (6 km, EW0102 dataset) in several MAR oceanic core complexes (which in some ways are similar to the tectonic setting of Rainbow: extreme topography, deep crustal and upper mantle rocks exposed on the seafloor) [*Canales et al.*, 2008]. Our recent experience with 6-km-streamer data shows that with those offsets we can image the upper ~500-1,700 m of the lithosphere (depending on sub-seafloor structure); therefore using a longer streamer up to 8 km will allow us deeper imaging (which in turn will result in smaller uncertainty in the shallower parts of the models), possibly up to ~2.5 km bsf. As a secondary objective, these long MCS profiles will also be processed using conventional 2-D seismic reflection techniques to provide some constraints (e.g., sediment thickness, structural images) for the 3D OBS refraction modeling/interpretation.

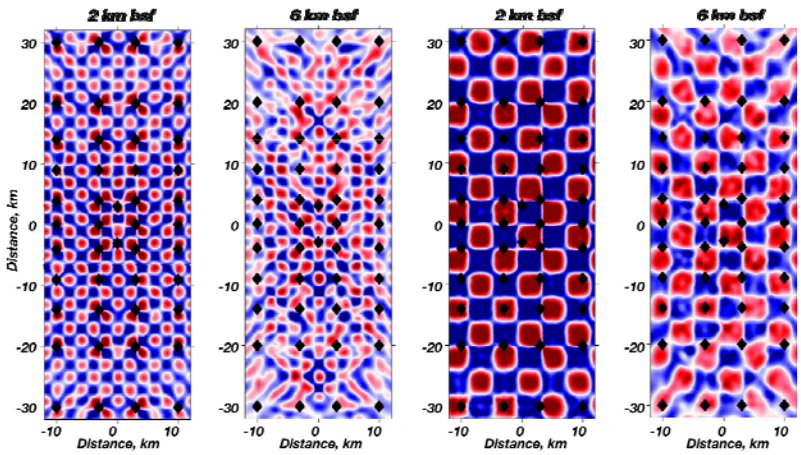

Fig 5. Checkerboard resolutions tests (2 km and 4 km patterns) illustrate the expected resolution at 2 km and 6 km depth bsf of the 3-D tomography experiment (MCS data not included). The repeating patterns of both 2 and 4 km sized checks are very well resolved. Even the 2 km pattern is well resolved at 6 km depth (within the central part of the study area around the Rainbow site) showing that imaging fine scale structure will be possible. Random Gaussian noise was added to the test data at a level consistent with past OBS experiments.

A second set of 10 28-km-long MCS profiles will be densely acquired across the Rainbow massif (**Figure 4-right**). The main purpose of these profiles will be to image faults across and beneath the flanks of the massif, and to image potential melt accumulation beneath the Rainbow massif. We note that imaging crustal melt lenses in this complex tectonic setting, if present, will be challenging, as it has been common in the past in the MAR [*Calvert*, 1995; *Detrick et al.*, 1990]. However modern seismic data has proved to be adequate for this purpose, as evidenced by the recent seismic imaging of a melt body beneath the Lucky Strike hydrothermal vent field [*Singh et al.*, 2006]. The dense spacing between profiles (1 km) will allow recognition of features from one profile to another easier, adding to the robustness of the interpretation. These 10 profiles are subdivided into two groups of different azimuths (E-W and NW-SW) across the main trends of fault and lineament patterns that crosscut the massif (see section 2) for optimal structural imaging. These MCS profiles will be processed using conventional 2-D seismic reflection techniques, and they will be used also for high-resolution 2D streamer tomography to characterize the lithological nature of the Rainbow massif.

[2] The primary purpose of the long SW-NE MCS lines is 2D high-resolution streamer tomography coincident with OBS profiles; being oriented along or across strike is of secondary importance for these profiles.

(3) Map the seismicity of the Rainbow area. We propose to acquire 6 months of passively recorded microearthquake data from the Rainbow site and its surroundings. It is now well established that microearthquake events are ubiquitous in records from seismometers deployed near deep-sea hydrothermal systems [*deMartin et al.*, 2007; *Golden et al.*, 2003; *McClain et al.*, 1993; *Riedesel et al.*, 1982; *Sohn et al.*, 1995, 1999b; *Tolstoy et al.*, 2002; *Wilcock*, 2001]. Such events can be used to investigate the thermal structure of the lithosphere, the stress regime, and map the faults that control local tectonics.

The causes of seismicity can be addressed by categorizing microearthquakes according to their waveform character, spectral content, and source mechanisms [e.g., *Lahr et al.*, 1994; *Sohn et al.*, 1999a, b]. We anticipate that the Rainbow area may exhibit seismicity indicative of both tectonic and thermal stresses, and our proposed network will allow us to distinguish between these different processes. Microearthquakes can delineate hydrothermal pathways by revealing the fault zones hosting fluid flow, and by identifying zones of increased permeability associated with stress concentrations. Microearthquakes also constrain thermal structure by delimiting the depth of the brittle-plastic transition within the study region.

We propose to place a subset of instruments around the vent site for obtaining detailed locations and depths of hydrothermal-related events and a broader distribution of stations to locate events associated with faulting over a larger region around the Rainbow massif (15 total short-period 4-component instruments) (**Figure 4-right**). Our network will provide a detailed study of the thermal and tectonic stresses beneath the hydrothermal field and within the NTD.

5. Logistics and Work Plan

Combining the MCS and OBS tomography experiments with the OBS passive-source deployment into one cruise minimizes costs by using one cruise leg aboard the R/V *Langseth* instead of two and shooting both experiments back-to-back, avoiding a duplication of costs for ship time, personnel, expendables and shipping. The study site is less than 2 days from Ponta Delgada, São Miguel Island in the Azores, a major mid-Atlantic port. This port has container ship service and it is routinely used by global-class oceanographic vessels. We require the R/V *Langseth* for 36 days of ship time (Table 1).

Table 1. Main Cruise Plan

Transit from port to 1st OBS site	2 days
Deploy 46 OBS	3.5
Shoot Refraction lines	7
Shoot MCS lines	6
Deploy/Recover streamer/gun for MCS	3
Recover 46 OBS	7
Redeploy 15 OBS	1.5
Transit to port	2
Contingency	4
Total	**36 days**
OBS recovery Cruise Plan	
Transit from port to 1st OBS site	2 days
Recover 15 OBS	3
Transit to port	2
Total	**7 days**

The OBS portion of the experiment consists of a single array of instruments positioned in a grid-like pattern. We will shoot to the 46 OBSs along about 1550 km of refraction, wide-angle reflection lines. Shots will be spaced 2.5 minutes apart (about 350 m at 4.5 knots). There is voluminous evidence that the best refraction data is obtained when water column reverberations are allowed to dissipate between shots. We request to use the short-period (4-component) instruments from the OBSIP instrument pool with the highest sampling rates available at the time of the experiment. We used current OBSIP guidelines for deployment times and a ship speed of 10 knots to calculate the time required for OBS operations (Table 1). The data will be entered in the IRIS databases shortly after the cruise and made available to the general community during the 2nd year.

The MCS component of the experiment will involve deploying of one 8-km-long streamer and one airgun array, and shooting along 7 80-km-long profiles trending SW-NE, 5 28-km-long profiles trending E-W, and 5 28-km-long profiles trending NW-SE (**Figure 4**). The long profiles will be collocated along the

OBS shooting profiles to maximize the synergy of the velocity modeling using the OBS and the MCS datasets. Shots will be fired every 37.5 m and recorded with the 640-channel streamer (receiver group spacing of 12.5 m) in 10-s-long records at a sampling rate of 2 ms. Sources and receivers will be navigated and accurately located using GPS receivers in the tail buoy and source floats, and compasses placed along the streamer.

Passive-source deployment for micro-earthquake study. After the active-source experiments are complete we will recover all of the OBS and then immediately redeploy (after downloading the data and resetting the instruments for long-term monitoring) 15 instruments for 6 months to detect micro-earthquakes. After that period any "ship of opportunity" can be used to recover these instruments (Table 1). The section of the MAR south of the Azores is a major site of scientific research. Portuguese and French investigators have been conducting cruises to the MoMAR area (which includes Lucky Strike and Rainbow sites) in recent years, and we expect they will continue to do so in the coming years.

6. Data Analysis

Our team has extensive experience successfully analyzing and interpreting active- and passive-source seismic data. In this section we summarize some of those methods that we will apply to the data. Initial data reduction (archiving, clock corrections, etc) is performed by the OBSIP instrument operators, who are also charged with depositing the data into the IRIS-DMC database.

6.1. OBS 3-D Tomography Data

We will construct 3-D tomographic images using a new method [*Dunn et al.*, 2005] that solves for 2- or 3-D velocity structure, reflector topography, and the magnitude and orientation of seismic anisotropy (hexagonal symmetry system). In this method, travel time picks are inputs to a 3-D tomographic inversion regularized by imposing spatial smoothing constraints on the roughness of the model parameters and optional damping constraints. The velocity images will be analyzed using theoretical and experimentally derived relations for the effects of temperature and melt fraction on seismic velocity to constrain thermal structure and melt distribution. We will use the OBS data to determine the degree of shallow, crack-induced anisotropy due to lithospheric stretching [e.g., *Barclay et al.*, 1998; *Dunn and Toomey*, 2001] and its orientation. We will quantitatively examine any trade-offs between isotropic velocity, reflector depths, and anisotropy. In follow-up work, we will model the finite-frequency effects on wave propagation and use finite-freq. methods to improve our analysis. We will integrate our results with the MCS data and other indicators of the thermal structure of the ridge (e.g. micro-earthquake distribution) to develop an integrated model of heat flux from its point of origin, up through the hydrothermal system.

6.2. Streamer 2-D Tomography Data

We will use the MCS data to obtain 2-D tomographic images of the shallow lithosphere (<2.5 km) [*Canales et al.*, 2008]. This method is most useful in areas where water depth is shallower than 3,200-3,000 (depending on subseafloor structure); our survey area in Rainbow is 95% shallower than 3,000 m and only a few small areas reach 3,200 m. Therefore we anticipate that streamer tomography will work well in the study area. We will form super-shot gathers by stacking several consecutive shot gathers to improve the signal-to-noise ratio prior to picking of the travel time arrivals. The MCS dataset will be over-sampled both in the source and receiver domains for ray-based travel time tomography. Spacing of sources and receivers (12.5 and 37.5 m, respectively) will be much denser than the first Fresnel zone at the seafloor, which limits the resolution of travel time tomography (e.g., 250 m for a dominant frequency of 30 Hz and seafloor depth of 2,500 m). Therefore travel time tomography of this dataset will require only travel time picks form a subset of the data. However we will pick travel times for all of the traces with first-arriving sub-crustal refractions because this ensures consistency across sources as well as across receivers. Although this may seem like an unnecessary time-consuming step, it can be done efficiently in

a timely manner using accurate semi-automated first-break picking routines commonly available in advanced MCS processing software (e.g., Focus by Paradigm^{TM}), as we did with the EW0102 dataset.

Travel time picks will be initially input into a 2-D tomographic inversion regularized by imposing spatial smoothing constraints on the roughness of the model. For streamer travel time tomography co-PI Canales has used in the past the software FAST developed by C. Zelt [*Zelt and Barton*, 1998]. The method accounts for the large topographic variations present in the area, as we confirmed in the core complex study. We will explore the possibility of using the same routines that will be applied to the 3-D OBS tomography study [*Dunn et al.*, 2005] but solving only for a 2-D structure. The resulting high-resolution velocity models will be interpreted in terms of shallow variations of the dominant lithologies, as it is expected that in the study area seafloor lithology will be highly heterogeneous, dominated primarily by volcanics, gabbros, and serpentinized peridotites. Our analysis of the EW0102 dataset together with in situ geological observations demonstrates that streamer tomography is a powerful tool to map the shallow distribution of gabbros and highly serpentinized peridotites [*Canales et al.*, 2008].

The 2-D MCS tomography results will be sub-sampled and interpolated onto the larger-scale 3-D OBS velocity volume used for the large-scale OBS tomography. This will impose good a priori constraints on the shallowmost structure that cannot be fully capture by the OBS array, which will be more sensitive to mid-crustal and deeper structures.

6.3. Seismic Reflection Imaging

The MCS profiles will be processed in a standard fashion including f-k and bandpass filtering, amplitude balancing, trace editing, geometry definition, sorting in common-mid point gathers, deconvolution, velocity analysis, normal move-out, muting, stack, and post-stack time/depth migration [e.g., *Yilmaz*, 1987]. Migration velocity models will be determined from the 2-D shallow tomography and 3-D OBS tomography studies. The reflection images will constrain the thickness of sediments wherever present (most likely within the basins flanking the Rainbow massif), potential major (detachment?) fault(s) associated with the uplift of the massif, small-scale faults across the Rainbow massif, potential melt lenses, and seismic Moho. As explained in the previous sections, abundant ultramafic rocks outcrop in the study area. The transition from serpentinized to unaltered mantle beneath Rainbow could be a sharp transition with abrupt increase in seismic velocity, as inferred at Atlantis Bank [*Muller et al.*, 1997], or a more gradual increase in seismic velocities [*Schroeder et al.*, 2002]. If the alteration front is sharp it should give rise to seismic reflections detectable by the MCS data. The combination of MCS and tomography models will help us distinguish between both hypotheses and determine the depth extent of mantle hydration beneath the vent field.

6.4. Earthquake Data

As a guide for the number of events we may expect to detect at Rainbow we use the recent microseismicity study of the TAG area (MAR 26°N) of *deMartin et al*. [2007]. Seismicity along a ~25 km stretch of the rift valley associated with the active TAG detachment fault occurred at a rate of ~80 events per day (for events with local magnitude $1 \leq M_L \leq 4$). If this rate is similar for the RHF, then we expect to catalog ~15,000 events during a 6-month deployment.

Upon receipt of the data we will enter it into an *Antelope* database and perform standard P and S-wave picking using the automatic algorithms in the *Antelope* system. This will be followed by manual checking of event picks and routine earthquake location using a 1-D velocity model, providing us with an in initial catalogue of events. Most passive earthquake studies have found that the *Antelope* picking algorithms do not perform well when applied to OBS data because of noise issues, and we fully expect this to be the case for Rainbow. We will address this issue by using a set of algorithms developed for the TAG dataset to refine the *P*- and *S*-wave picks using spectral techniques and residual values for nominal

1-D hypocenter locations. We will then use a grid-search technique to generate more accurate hypocentral estimates with the refined set of body wave arrival picks. The grid search technique is computationally expensive, but given the speed of modern computers this is no longer a problem. The grid search technique also provides much more robust error estimates compared to linearized methods.

The next phase of data analysis will involve waveform cross-correlation and relative relocation. The value of using waveform cross-correlation and relative relocation for clarifying the spatial distribution of earthquakes has been well established [e.g., *Gillard et al.*, 1996; *Got et al.*, 1994; *Got and Okubo*, 2003; *Rubin et al.*, 1998; *Wolfe et al.*, 2003, 2004]. Waveform cross-correlation will be carried out in two steps. First, we will carry out a standard cross-correlation analysis using bandpass-filtered waveforms, including the use of cross-spectral phase for sub-sample alignment for highly correlated waveform pairs [e.g., *Rowe et al.*, 2004]. Next, we will reprocess the waveforms using the bispectrum verification procedure [*Du et al.*, 2004], which can increase both the quantity and reliability of waveform lags by checking that the standard cross-correlation lag agrees with the bispectrum lag. Using the *Antelope* results as initial locations, the differential times will be used with *hypoDD* [*Waldhauser and Ellsworth*, 2000] to relocate self-similar events.

The analysis of the data will also include categorizing event types. We will calculate focal mechanisms for all events with sufficiently clear *P*-wave polarities and adequate azimuthal coverage, and will look for correlations between event location, event type (based on spectral content), and event mechanism. Event locations and types/mechanisms will provide us with an accurate catalogue of events for examining tectonic and hydrothermal processes. If sufficient focal mechanism data are available, we will invert for the regional stress field [e.g., *Giampiccolo et al.*, 1999; *Jolly et al.*, 1994; *Moran*, 2003; *Prejean et al.*, 2002; *Sánchez et al.*, 2004].

Division of Tasks. **J. Pablo Canales** (WHOI) will coordinate the MCS part of the experiment, leading the MCS data processing, reflection imaging, and shallow 2D tomography modeling. **Robert Dunn** (U. Hawaii) will coordinate the OBS deployments and supervise the active-source tomography OBS data analysis. **Robert Reves-Sohn** (WHOI) will supervise the passive OBS deployment/recovery for microearthquake monitoring and will lead the analysis of the microseismicity data. Data and results will be combined at different stages of the analysis as needed to ultimately form integrated, high-resolution sub-surface images of the Rainbow area.

7. Broader Impacts

This project will make valuable contributions to scientific infrastructure. New seismic models will be developed and ultimately distributed for use by the community via publication and PI websites. The data sets we collect are substantive and each will be made available to the broader community via the IRIS data management center and will provide productive research in many areas for years to come. The proposed research will play a role in accomplishing the goals of the RIDGE2000 science program, a NSF-funded program focused on the interdisciplinary investigation of fundamental ridge-related problems on scales ranging from mantle convection to microbe activity. In addition, the section of the MAR south of the Azores is a major site of international scientific interest. For example, French investigators have conducted recently several cruises to the MoMAR area (including Rainbow) and our work will broadly impact those studies.

Development of human resources in the form of graduate and undergraduate student training is an important outgrowth of this proposal. This study will form part of the Ph.D. thesis research project of UH-SOEST and MIT/WHOI Joint Program graduate students, who will be trained in different seismic disciplines. The PIs will incorporate undergraduate interns in various aspects of the work, from sea going to data analysis. These students will gather and analyze data and will be introduced to earthquake analysis and seismic imaging methods. Most U. of Hawaii undergraduates are residents of Hawaii and represent an

ethnically diverse student body (19% Caucasian, 9% Filipino, 11% Native Hawaiian, 23% Japanese, 38% mixed or other). It is intended that the laboratory and scholarly activities of the undergraduates and PIs will deepen the participation of these underrepresented groups in earth science. We will work with the SOEST outreach coordinator and contribute results and images for their K-12 and general public efforts. In addition, Dunn maintains a very popular museum-style display on the UH campus that provides general-public type seismic information (e.g., info. on plate tectonics, historical and near-real-time seismicity, both local and global).

8. Results from Prior Support

J.P. Canales. *OCE-0621660 (B. Tucholke, co-P.I.), Shallow seismic structure of the ocean crust and its correlation with seafloor lithologies on the Kane megamullion, Mid-Atlantic 23° 20'-23° 40'N, $280,135, 09/01/2006-08/31/2008.* This project consisted on a detailed study on Kane megamullion, where a broad cross section of ocean crust and upper mantle is interpreted to have been exposed by long-lived detachment faulting. Our objectives were to integrate high-resolution shallow seismic tomography models with available geological samples in order to investigate fundamental questions about the segment-scale geological and geophysical structure of ocean crust formed under conditions of limited magma supply, and to provide data necessary both to properly site proposed IODP boreholes and to interpret eventual drilling results. We performed high-resolution travel-time seismic tomography inversions of MCS data acquired with a 6-km-long streamer to obtain the detailed P-wave velocity structure in the upper 500-1000 meters of basement and use this information to interpret lateral and vertical lithological variations in the crust by using constraints provided by an extensive suite of lithological data. We also obtained the seismic structure of two other MAR core complexes (Atlantis Massif and Dante's Domes) to make comparisons among the different sites and provide constraints on fundamental features of core complex formation and detachment faulting. Our results show that large lateral variations in P-wave velocity occur within the upper ~0.5-1.7 km of the lithosphere. We observe good correlations between velocity structure and lithology as documented by *in situ* geological samples, and we use these correlations to show that gabbros are heterogeneously distributed as large (10s of km^2) bodies within serpentinized peridotites. Neither the gabbros nor the serpentinites show any systematic distribution with respect to along-isochron position within the enclosing spreading segment, indicating that melt extraction from the mantle is not necessarily focused at segment centers, as has been commonly inferred. Gabbros are consistently present toward the terminations of the detachment faults, suggesting that they may have been emplaced by late-stage decompression melting during footwall exhumation. Detailed seismic studies of the kind carried out in this project have tremendous potential to elucidate the internal structure of the crust and upper mantle and thus to understand the tectonic and magmatic processes by which they were emplaced. This project has resulted in 3 AGU abstracts, one Ph.D. thesis chapter, and three peer-reviewed papers [*Blackman et al.*, 2009; *Canales et al.*, 2008; *Xu et al.*, 2009]. Data are available to the public through the Marine Seismic Data Center (www.ig.utexas.edu/sdc).

R. Reves-Sohn and J.P. Canales. *OCE-0137329 (S. Humphris, co-P.I.), Seismicity, Structure, and Fluid Flow of the TAG Hydrothermal System, $480,806, 03/01/2003-02/28/2006.* This project was focused on the crustal architecture of the TAG segment in the Mid-Atlantic Ridge (26°N) and the hydrogeology of the TAG hydrothermal system. The STAG experiment was carried out over the course of four research legs stretching from June 2003 to November 2004. We conducted simultaneous observations of seismic activity, exit-fluid temperatures, and tidal pressures at the TAG mound during an 8-month period, as well as an active-source seismic refraction experiment. Hypocenters from 19,232 microearthquakes observed during the eight-month OBS deployment, together with the seismic refraction data, reveal for the first time the geometry and seismic character of an active oceanic detachment fault. The microseismicity forms an ~15-km-long, dome-shaped fault surface that penetrates to depths >7 km below the seafloor on a steeply dipping (~70°) interface. A tomographic model of compressional-wave velocities demonstrates that lower crustal rocks are being exhumed in the detachment footwall, which appears to roll over to a

shallow dip of 20° ± 5° and become aseismic at a depth of ~3 km. The seismic tomography results also show that hydrothermal circulation at TAG is not driven by energy extracted from shallow or mid-crustal magmatic intrusions. Instead, the TAG hydrothermal field is underlain by rocks with high seismic velocities typical of lower crustal gabbros and partially serpentinized peridotites at depth as shallow as 1 km, and we find no evidence for low seismic velocities associated with mid-crustal magma chambers. Our tomographic images constrain the complex, dome-shaped subsurface geometry of a young oceanic detachment fault. Our results suggest that hydrothermal fluids at the TAG field exploit the detachment fault to extract heat from a region near the crust-mantle interface over long periods of time. To date, this project has resulted in one Ph.D. thesis chapter, several AGU abstracts, and 4 papers [*Canales et al.*, 2007; *deMartin et al.*, 2007; *Sohn*, 2007a; b]. Data are available to the public through the IRIS on-line database (www.iris.edu).

R. Dunn. *OCE-0203228, Three-Dimensional Velocity Structure and Crustal Thickness Beneath a Slow-Spreading Ridge, $174,838, 01/0102-12/31/05*. This grant funded a three-dimensional seismic tomography study of a section of the Mid-Atlantic Ridge near 35˚N. For segments of slow-spreading mid-ocean ridges bounded by tectonic offsets, several observations indicate that the melt flux to the ridge is focused in the mantle and preferentially delivered to the segment center. By this view, there should exist a three-dimensional thermal structure in the newly forming lithosphere; seafloor spreading should be more magmatically accommodated near a segment's midsection and more tectonically accommodated near the ends. To test this model, we gathered seismic refraction and wide-angle reflection data from several active-source experiments that occurred along the Mid-Atlantic Ridge near 35˚N and using travel times of 31,405 *P*, 17,711 *PmP*, and 11,716 *Pn* arrivals recorded by 49 ocean bottom instruments we constructed three-dimensional anisotropic tomographic images of the crust and upper mantle velocity structure and crustal thickness. The tomographic images reveal anomalously thick crust (8-9 km) and a low-velocity "bulls-eye", from 4-10 km depth, beneath the center of the ridge segment. The velocity anomaly is indicative of high temperatures and a small amount of melt (up to 5%) and likely represents the current magma plumbing system for melts ascending from the mantle. In addition, at the segment center, seismic anisotropy in the lower crust indicates that the crust is composed of partially molten dikes that are surrounded by regions of hot rock with little or no melt fraction. Our results indicate that mantle melts are focused at mantle depths to the segment center and that melt is delivered to the crust via dikes in the lower crust. Our results also indicate that the segment ends are colder, receive a reduced magma supply, and undergo significantly greater tectonic stretching than the segment center [*Dunn et al.*, 2005].

References.

Allen, D. E., and W. E. Seyfried (2004), Serpentinization and heat generation: constraints from Lost City and Rainbow hydrothermal systems, *Geochimica et Cosmochimica Acta*, *68*, 1347-1355.

Baker, E. T., and C. R. German (2004), On the global distribution of hydrothermal vent fields, in *Mid-Ocean Ridges: Hydrothermal Interactions Between the Lithosphere and Oceans*, edited by C. R. German, et al., pp. 245-266, AGU, Washington, D.C.

Barclay, A. H., D. R. Toomey, and S. C. Solomon (1998), Seismic structure and crustal magmatism at the Mid-Atlantic Ridge, 35°N, *J. Geophys. Res.*, *103*, 17,827-817,844.

Barriga, F., et al. (1998), Discovery of the Saldanha hydrothermal field on the FAMOUS segment of the MAR (36°30'N), *Eos Trans. AGU*, *79*, Fall Meet. Suppl., F67.

Bel'tenev, V., et al. (2005), New hydrothermal sites at 13°N, Mid-Atlantic Ridge, *InterRidge News*, *14*, 14-16.

Blackman, D. K., J. P. Canales, and A. J. Harding (2009), Geophysical signatures of oceanic core complexes, *Geophys. J. Int.*, *178*, 593–613.

Blackman, D. K., B. Ildefonse, B. E. John, Y. Ohara, D. J. Miller, C. J. MacLeod, and Expedition 304/305 Scientists (2006), Oceanic Core Complex Formation, Atlantis Massif, *Proc. IODP*, *304/305*, doi: 10.2204/iodp.proc.304305.302006.

Blackman, D. K., et al. (2002), Geology of the Atlantis Massif (Mid-Atlantic Ridge, 30°N): Implications for the evolution of an ultramafic oceanic core complex, *Mar. Geophys. Res.*, *23*, 443-469.

Bonatti, E. (1976), Serpentinite protrusions in the oceanic crust, *Earth Planet. Sci. Lett.*, *32*, 107-113.

Buck, W. R. (1988), Flexural rotation of normal faults, *Tectonics*, *7*, 959-973.

Calvert, A. J. (1995), Seismic evidence for a magma chamber beneath the slow-spreading Mid-Atlantic Ridge, *Nature*, *377*, 410-414.

Calvert, A. J., M. A. Fisher, S. Y. Johnson, and the SHIPS Working Group (2003), Along-strike variations in the shallow seismic velocity structure of the Seattle fault zone: Evidence for fault segmentation beneath Puget Sound, *J. Geophys. Res.*, *108*, 2005, doi:2010.1029/2001JB001703.

Canales, J. P., R. S. Detrick, J. Lin, J. A. Collins, and D. R. Toomey (2000), Crustal and upper mantle seismic structure beneath the rift mountains and across a non-transform offset at the Mid-Atlantic Ridge (35°N), *J. Geophys. Res.*, *105*, 2699-2719.

Canales, J. P., S. C. Singh, R. S. Detrick, S. M. Carbotte, A. J. Harding, G. M. Kent, J. B. Diebold, J. Babcock, and M. R. Nedimović (2006), Seismic evidence for variations in axial magma chamber properties along the southern Juan de Fuca Ridge, *Earth Planet. Sci. Lett.*, *246*, 353-366.

Canales, J. P., R. A. Sohn, and B. deMartin (2007), Crustal structure of the Trans-Atlantic Geotraverse (TAG) segment (Mid-Atlantic Ridge, 26° 10'N): Implications for the nature of hydrothermal circulation and detachment faulting at slow spreading ridges, *Geochem., Geophys., Geosyst.*, *8*, Q08004, doi:08010.01029/02007GC001629.

Canales, J. P., B. E. Tucholke, M. Xu, J. A. Collins, and D. L. Dubois (2008), Seismic evidence for large-scale compositional heerogeneity of oceanic core complexes, *Geochem., Geophys., Geosyst.*, *9*, Q08002, doi:08010.01029/02008GC002009.

Cann, J. R., M. R. Strens, and A. Rice (1985), A simple magma-driven thermal balance model for the formation of volcanogenic massive sulphides, *Earth Planet. Sci. Lett.*, *76*, 123-134.

Cannat, M., J. R. Cann, and J. MacLennan (2004), Some hard rock constraints on the supply of heat to mid-ocean ridges, in *Mid-ocean ridges: Hydrothermal interactions between the*

lithosphere and the oceans, edited by C. R. German, et al., pp. 111-149, AGU, Washington, D.C.

Cannat, M., et al. (1995), Thin crust, ultramafic exposures, and rugged faulting patterns at the Mid-Atlantic Ridge (22°-24°N), *Geology*, *23*, 49-52.

Charlou, J. J., J. P. Donval, Y. Fouquet, P. Jean Baptiste, and N. Holm (2002), Geochemistry of high H2 and CH4 vent fluids issuing from ultramafic rocks at the Rainbow hydrothermal field (36°14'N, MAR), *Chemical Geology*, *191*, 345-359.

Coleman, R. G. (1971), Petrological and geophysical nature of serpentinites, *Geological Society of America Bulletin*, *82*, 897-918.

deMartin, B. J., R. Reves-Sohn, J. P. Canales, and S. E. Humphris (2007), Kinematics and geometry of active detachment faulting beneath the Trans-Atlantic Geotraverse (TAG) hydrothermal field on the Mid-Atlantic Ridge, *Geology*, *35*, 711-714.

Desbruyères, D., M. Biscoiti, J.-C. Caprais, and et al. (2001), Variations in deep-sea hydrothermal vent communities on the Mid-Atlantic ridge near the Azores plateau, *Deep Sea Research Part I*, *48*, 1325-1346.

Detrick, R. S., J. C. Mutter, P. Buhl, and I. I. Kim (1990), No evidence from multichannel reflection data for a crustal magma chamber in the MARK area on the Mid-Atlantic Ridge, *Nature*, *347*, 61-64.

Dick, H. J. B., J. Lin, and H. Schouten (2003), An ultraslow-spreading class of ocean ridge, *Nature*, *426*, 405-412.

Dick, H. J. B., et al. (2000), A long in situ section of the lower ocean crust: results of ODP Leg 176 drilling at the Southwest Indian ridge, *Earth Planet. Sci. Lett.*, *179*, 31-51.

Du, W., C. H. Thurber, and D. Eberhart-Phillips (2004), Earthquake relocation using cross-correlation time delay estimates verified with the bispectrum method, *Bulletin of the Seismological Society of America*, *94*, 856-866.

Dunn, R. A., V. Lekic, R. S. Detrick, and D. R. Toomey (2005), Three-dimensional seismic structure of the Mid-Atlantic Ridge (35°N): Evidence for focused melt supply and lower crustal dike injection, *J. Geophys. Res.*, *110*, B09101, doi:09110.01029/02004JB003473.

Dunn, R. A., and D. R. Toomey (1997), Seismological evidence for the three-dimensional melt migration beneath the East Pacific Rise, *Nature*, *388*, 259-262.

Dunn, R. A., and D. R. Toomey (2001), Crack-induced seismic anisotropy in the oceanic crust across the East Pacific Rise (9° 30'N), *Earth Planet. Sci. Lett.*, *189*, 9-17.

Dunn, R. A., D. R. Toomey, R. S. Detrick, and W. S. D. Wilcock (2001), Continuous mantle melt supply beneath an overlapping spreading center on the East Pacific Rise, *Science*, *291*, 1955-1958.

Dunn, R. A., D. R. Toomey, and S. C. Solomon (2000), Three-dimensional seismic structure and physical properties of the crust and shallow mantle beneath the East Pacific Rise at 9° 30'N, *J. Geophys. Res.*, *105*, 23,537-523,555.

Dyment, J., Y. Fouquet, P. Gente, B. Ildefonse, R. Thibaud, E. Hoise, D. Bissessur, and V. Yatheesh (2008), Deep-sea investigations on hydrothermal site Rainbow (MAR 36°14'N), *Eos Trans. AGU*, *89*, Fall Meet. Suppl., Abstract T43B-2026.

Escartín, J., C. Mével, C. J. MacLeod, and A. M. McCaig (2003), Constraints on deformation conditions and the origin of oceanic detachments: The Mid-Atlantic Ridge core complex at 15°45'N, *Geochem., Geophys., Geosyst.*, *4*, 1067, doi:1010.1029/2002GC000472.

Escartín, J., D. K. Smith, J. Cann, H. Schouten, C. H. Langmuir, and S. Escrig (2008), Central role of detachment faults in accretion of slow-spreading oceanic lithosphere, *Nature*, *455*, 790-794.

Fouquet, Y., J. L. Charlou, and F. Barriga (2002), Modern seafloor hydrothermal deposits hosted in ultramafic rocks, *Geol. Soc. Am. Abstracts with Programs*, *34*, 194-197.

Fouquet, Y., et al. (1997), Discovery and first submersible on the Rainbow hydrothermal field on the MAR (36°14'N), *Eos Trans. AGU*, *78*, 832.

Fouquet, Y., H. Ondreas, J. L. Charlou, J. P. Donval, J. Radford-Knoery, I. Costa, N. Lourenço, and M. K. Tivey (1995), Atlantic lava lakes and hot vents, *Nature*, *377*, 201.

Früh-Green, G. L., D. S. Kelley, S. M. Bernasconi, J. A. Karson, K. A. Ludwig, D. A. Butterfield, C. Boschi, and G. Proskurowski (2003), 30,000 years of hydrothermal activity at the Lost City vent field, *Science*, *301*, 495-498.

Gaill, F., et al. (2007), Cruise MoMARDREAM-Naut and other MoMAR experiments at Rainbow and Lucky Strike in Summer 2007, *InterRidge News*, *16*, 15-16.

Gente, P., R. Thibaud, J. Dyment, Y. Fouquet, B. Ildefonse, E. Hoise, D. Bissessur, and V. Yatheesh (2008), High resolution topography of the Rainbow hydrothermal area, Mid-Atlantic Ridge, 36°14'N, *Eos Trans. AGU*, *89*, Fall Meet. Suppl., Abstract T43B-2027.

German, C. R., and J. Lin (2004), The thermal structure of the oceanic crust, ridge-spreading and hydrothermal circulation: how well do we understand their inter-connections?, in *Mid-Ocean Ridges: Hydrothermal Interactions Between the Lithosphere and Oceans*, edited by C. R. German, et al., pp. 1-18, AGU, Washington, D.C.

German, C. R., and L. M. Parson (1998), Distributions of hydrothermal activity along the Mid-Atlantic Ridge: interplay of magmatic and tectonic controls, *Earth Planet. Sci. Lett.*, *160*, 327-341.

German, C. R., L. M. Parson, and H. S. Team (1996), Hydrothermal exploration near the Azores Triple Junction: tectonic control of venting at slow-spreading ridges, *Earth Planet. Sci. Lett.*, *138*, 93-104.

Giampiccolo, E., C. Musumeci, S. Malone, S. Gresta, and E. Privitera (1999), Seismicity and stress tensor inversion n the Central Washington Cascade Mountains, *Bulletin of the Seismological Society of America*, *89*, 811-821.

Gillard, D., A. M. Rubin, and P. Okubo (1996), Highly concentrated seismicity caused by deformation of Kilauea's deep magma system, *Nature*, *384*, 343-346.

Golden, C. E., S. C. Webb, and R. A. Sohn (2003), Hydrothermal microearthquake swarms beneath active vents at Middle Valley, northern Juan de Fuca Ridge, *J. Geophys. Res.*, *108*, 2027, doi: 2010.1029/2001JB000226.

Got, J.-L., J. Fréchet, and F. W. Klein (1994), Deep fault plane geometry inferred from multiplet relative relocation beneath the south flank of Kilauea, *J. Geophys. Res.*, *99*, 15,375-315,386.

Got, J.-L., and P. Okubo (2003), New insights into Kilauea's volcano dynamics brought by large-scale relative relocation of microearthquakes, *J. Geophys. Res.*, *108*, 2337, doi:2310.1029/2002JB002060.

Gràcia, E., D. Bideau, R. Hekinian, Y. Lagabrielle, and L. M. Parson (1997), Along-axis magmatic oscillations and exposures of ultramafics rocks in a second-order segment of the Mid-Atlantic Ridge (33°43'N to 34°07'N), *Geology*, *25*, 1059-1062.

Gràcia, E., J.-L. Charlou, J. Radford-Knoery, and L. M. Parson (2000), Non-transform offsets along the Mid-Atlantic Ridge south of the Azores (38°N-34°N): ultramafic exposures and hosting of hydrothermal vents, *Earth Planet. Sci. Lett.*, *177*, 89-103.

Grindlay, N. R., and P. J. Fox (1993), Lithospheric stresses associated with non-transform offsets of the Mid-Atlantic Ridge: implications for a finite element analysis, *Tectonics*, *12*, 982-1003.

Grindlay, N. R., P. J. Fox, and K. C. MacDonald (1991), Second-order axis discontinuities in the South Atlantic: Morphology, structure, and evolution, *Mar. Geophys. Res.*, *13*, 21-50.

Haymon, R. M., D. J. Fornari, M. H. Edwards, S. M. Carbotte, D. J. Wright, and K. C. Macdonald (1991), Hydrothermal vent distribution along the East Pacific Rise crest (9°09'-54'N) and its relationship to magmatic and tectonic processes on fast-spreading mid-ocean ridges, *Earth Planet. Sci. Lett.*, *104*, 513-534.

Holm, N. G., and J. L. Charlou (2001), Initial indications of abiotic formation of hydrocarbons in the Rainbow ultramafic hydrothermal system, Mid-Atlantic Ridge, *Earth Planet. Sci. Lett.*, *191*, 1-8.

Humphris, S. E., et al. (1995), The internal structure of an active sea-floor massive sulphide deposit, *Nature*, *377*, 713-716.

Ildefonse, B., M. Andreani, E. Hoise, V. Ballu, J. Escartín, J. Dyment, F. Gaill, and T. Fouquet (2007a), Further geological sampling around the Rainbow hydrothermal site, Mid-Atlantic Ridge, *Eos Trans. AGU*, *88*, Fall Meet. Suppl., Abstract T53B-1306.

Ildefonse, B., D. K. Blackman, B. E. John, Y. Ohara, D. J. Miller, C. J. MacLeod, and I. O. E. S. Party (2007b), Oceanic core complexes and crustal accretion at slow-spreading ridges, *Geology*, *35*, 623-626.

Ildefonse, B., Y. Fouquet, E. Hoise, J. Dyment, P. Gente, R. Thibaud, D. Bissessur, and V. Yatheesh (2008), Geological mapping of the Rainbow Massif, Mid-Atlantic Ridge, 36°14'N, *Eos Trans. AGU*, *89*, Fall Meet. Suppl., Abstract T43B-2028.

Jolly, A. D., R. A. Page, and J. A. Power (1994), Seismicity and stress in the vicinity of Mount Spurr volcano, south central Alaska, *J. Geophys. Res.*, *99*, 15,305-315,318.

Kelemen, P. B., E. Kikawa, D. J. Miller, and Shipboard Scientific Party (2004), *Proc. ODP Init. Rep.*, *209*, doi: 10.2973/odp.proc.ir.2209.2004.

Krasnov, S., G. Cherkashev, I. Poroshina, Y. Fouquet, D. Prieur, and A. Ashadze (1996), 15°N Mid-Atlantic Ridge Logatchev hydrothermal field, paper presented at FARA-InterRidge Mid-Atlantic Ridge Symposium.

Lahr, J. C., B. A. Chouet, C. D. Stephens, J. A. Power, and R. A. Page (1994), Earthquake classification, location, and error analysis in a volcanic environment: implications for the magmatic system of the 1989-1990 eruptions at Redoubt Volcano, Alaska, *Journal of Volcanology and Geothermal Research*, *62*, 137-151.

Langmuir, C., et al. (1997), Hydrothermal vents near a mantle hot spot: the Lucky Strike vent field at 37°N on the Mid-Atlantic Ridge, *Earth Planet. Sci. Lett.*, *148*, 69-91.

Lin, J., G. M. Purdy, H. Schouten, J.-C. Sempéré, and C. Zervas (1990), Evidence from gravity data for focused magmatic accretion along the Mid-Atlantic Ridge, *Nature*, *344*, 627-632.

Macdonald, A. H., and W. S. Fyfe (1985), Rate of serpentinization in seafloor environments, *Tectonophysics*, *116*, 123-135.

McCaig, A. M., R. A. Cliff, J. Escartín, A. E. Fallick, and C. J. MacLeod (2007), Oceanic detachment faults focus very large volumes of black smoker fluids, *Geology*, *35*, 935-938.

McClain, J. S., M. L. Begnaud, M. A. Wright, J. Fondrk, and G. K. Von Damm (1993), Seismicity and tremor in a submarine hydrothermal field: the northern Juan de Fuca Ridge, *Geophys. Res. Lett.*, *20*, 1883-1886.

Moran, S. C. (2003), Multiple seismogenic processes for high-frequency earthquakes at Katmai National Park, Alaska: Evidence from stress tensor inversions of fault-plane solutions, *Bulletin of the Seismological Society of America*, *93*, 94-108.

Muller, M. R., C. J. Robinson, T. A. Minshull, R. S. White, and M. J. Bickle (1997), Thin crust beneath ocean drilling program borehole 735B at the Southwest Indian Ridge?, *Earth Planet. Sci. Lett.*, *148*, 93-107.

O'Brien, D., M. Carton, D. Eardly, and J. W. Patching (1998), In situ filtration and preliminary molecular analysis of microbial biomass from the Rainbow hydrothermal plume at 36°15'N on the Mid-Atlantic Ridge, *Earth Planet. Sci. Lett.*, *157*, 223-231.

Phipps Morgan, J., and D. W. Forsyth (1988), Three-dimensional flow and temperature perturbations due to a transform offset: Effects on oceanic crustal and upper mantle structure, *J. Geophys. Res.*, *93*, 2955-2966.

Prejean, S., W. Ellsworth, M. Zoback, and F. Waldhauser (2002), Fault structure and kinematics of the Long Valley Caldera region, California, revealed by high-accuracy earthquake

hypocenters and focal mechanism stress inversions, *J. Geophys. Res.*, *107*, 2355, doi:2310.1029/2001JB001168.

Riedesel, M., J. A. Orcutt, K. C. MacDonald, and J. S. McClain (1982), Microearthquakes in the Black Smoker hydrothermal field, East Pacific Rise at 21°N, *J. Geophys. Res.*, *87*, 10,613-610,623.

Rowe, C. A., C. H. Thurber, and R. A. White (2004), Dome growth behavior at Soufriere Hills Volcano, Montserrat, revealed by relocation of volcanic event swarms, 1995–1996, *Journal of Volcanology and Geothermal Research*, *134*, 199-221.

Rubin, A. M., D. Gillard, and J.-L. Got (1998), A reinterpretation of seismicity associated with the January 1983 dike intrusion at Kilauea Volcano, Hawaii, *J. Geophys. Res.*, *103*, 10,003-010,015.

Sánchez, J. J., M. Wyss, and S. R. McNutt (2004), Temporal-spatial variations of stress at Redoubt volcano, Alaska, inferred from inversion of fault plane solutions, *Journal of Volcanology and Geothermal Research*, *130*, 1-30.

Schroeder, T., B. E. John, and B. R. Frost (2002), Geologic implications of seawater circulation through peridotite exposed at slow-spreading mid-ocean ridges, *Geology*, *30*, 367-370.

Singh, S. C., et al. (2006), Discovery of a magma chamber and faults beneath a Mid-Atlantic Ridge hydrothermal field, *Nature*, *442*, 1029-1032.

Singh, S. C., G. M. Kent, J. S. Collier, A. J. Harding, and J. A. Orcutt (1998), Melt to mush variations in crustal magma properties along the ridge crest at the southern East Pacific Rise, *Nature*, *394*, 874-878.

Smith, D. K., J. R. Cann, and J. Escartín (2006), Widespread active detachment faulting and core complex formation near 13°N on the Mid-Atlantic Ridge, *Nature*, *442*, doi:10.1038/nature04950.

Sohn, R. A. (2007a), Stochastic analysis of exit fluid temperature records from the active TAG hydrothermal mound (Mid-Atlantic Ridge, 26 N): 1. Modes of variability and implications for subsurface flow, *J. Geophys. Res.*, *112*, B07101, doi:07110.01029/02006JB004435.

Sohn, R. A. (2007b), Stochastic analysis of exit-fluid temperature records from the active TAG hydrothermal mound (Mid-Atlantic Ridge, 26°N): 2. Hidden Markov models of flow episodes, *J. Geophys. Res.*, *112*, B09102, doi:09110.01029/02007JB004961.

Sohn, R. A., W. C. Crawford, and S. C. Webb (1999a), Local seismicity following the 1998 eruption of axial volcano, *Geophys. Res. Lett.*, *26*, 3433-3436.

Sohn, R. A., J. A. Hildebrand, and S. C. Webb (1999b), A microearthquake survey of the high-temperature vent fields on the volcanically active East Pacific Rise (9° 50'N), *J. Geophys. Res.*, *104*, 25,367-325,377.

Sohn, R. A., J. A. Hildebrand, S. C. Webb, and C. G. Fox (1995), Hydrothermal microseismicity at the Megaplume site on the Southern Juan de Fuca Ridge, *Bulletin of the Seismological Society of America*, *85*, 775-783.

Thurnherr, A. M., and K. J. Richards (2001), Hydrography and high-temperature heat flux of the Rainbow hydrothermal site (36°14'N, Mid-Atlantic Ridge), *J. Geophys. Res.*, *106*, 9411-9426.

Thurnherr, A. M., K. J. Richards, C. R. German, and G. F. Lane-Serff (2002), Flow and mixing in the rift valley of the Mid-Atlantic Ridge, *Journal of Physical Oceanography*, *32*, 1763-1778.

Tolstoy, M., F. L. Vernon, J. A. Orcutt, and F. K. Wyatt (2002), Breathing of the seafloor: Tidal correlations of seismicity at Axial volcano, *Geology*, *30*, 503-506.

Tucholke, B. E., and J. Lin (1994), A geological model for the structure of ridge segments in slow spreading ocean crust, *J. Geophys. Res.*, *99*, 11,937-911,958.

Van Ark, E., et al. (2007), Seismic structure of the Endeavour segment, Juan de Fuca Ridge: Correlations with seismicity and hydrothermal activity, *J. Geophys. Res.*, *112*, B02401, doi:02410.01029/02005JB004210.

Von Damm, K. L. (1990), Seafloor hydrothermal activity: black smokers and chimneys, *Annual Review of Earth and Planetary Science*, *18*, 173-204.

Waldhauser, F., and W. L. Ellsworth (2000), A double-difference earthquake location algorithm: Method and application to the northern Hayward fault, *Bulletin of the Seismological Society of America*, *90*, 1353-1368.

Wilcock, W. S. D. (2001), Tidal triggering of microearthquakes on the Juan de Fuca Ridge, *Geophys. Res. Lett.*, *28*, 3999-4002.

Wilcock, W. S. D., and J. R. Delaney (1996), Mid-ocean ridge sulfide deposits: Evidence for heat extraction from magma chambers or cracking fronts?, *Earth Planet. Sci. Lett.*, *145*, 49-64.

Wolfe, C. J., P. B. Okubo, G. Ekström, M. Nettles, and P. M. Shearer (2004), Characteristics of deep (>=13 km) Hawaiian earthquakes and Hawaiian earthquakes west of 155.55°W, *Geochem., Geophys., Geosyst.*, *5*, Q04006, doi:04010.01029/02003GC000618.

Wolfe, C. J., P. B. Okubo, and P. M. Shearer (2003), Mantle fault zone beneath Kilauea volcano, Hawaii, *Science*, *300*, 478-480.

Xu, M., J. P. Canales, B. E. Tucholke, and D. L. Dubois (2009), Heterogeneous seismic velocity structure of the upper lithosphere at Kane oceanic core complex, Mid-Atlantic Ridge 23°17'N-23°37'N, *Geochem., Geophys., Geosyst.*, in press.

Yilmaz, Ö. (1987), *Seismic Data Processing*, 526 pp., Investigations in Geophysics, vol. 2, Society of Exploration Geophysicists, Tulsa, OK.

Zelt, B. C., B. Taylor, J. R. Weiss, A. M. Goodliffe, M. Sachpazi, and A. Hirn (2004), Streamer tomography velocity models for the Gulf of Corinth and Gulf of Itea, Greece, *Geophys. J. Int.*, *159*, 333-346.

Zelt, C. A., and P. J. Barton (1998), Three-dimensional seismic refraction tomography: A comparison of two methods applied to data from the Faeroe Basin, *J. Geophys. Res.*, *103*, 7187-7210.